NASA TT F-9744

EXPERIMENTAL AND THEORETICAL RESULTS ON HEAT TRANSFER AT THE ANGLE OF ATTACK OF SWEPT WINGS IN HYPERSONIC FLIGHT

Jacques Valensi, Roger Michel and Daniel Guffroy

Translation of "Résultats éxperimentaux et théoriques sur le transfert de chaleur au bord d'attaque des ailes à forte flèche en hypersonique" Paper presented at the Meeting of the Fluid Mechanics Group, AGARD, Naples, May 10-14, 1965. Office National d'Etudes et de Recherches Aerospatiales (ONERA-TP 217, 1965)

NATIONAL AERONAUTICS AND SPACE ADMINISTRATION
WASHINGTON NOVEMBER 1965

EXPERIMENTAL AND THEORETICAL RESULTS ON HEAT TRANSFER AT THE ANGLE OF ATTACK OF SWEPT WINGS IN HYPERSONIC FLIGHT

Jacques Valensi, Roger Michel, and Daniel Guffroy

ABSTRACT

11951

An experimental and theoretical study of cooling and heat /1* transfer at the leading edge of hypersonic wings at Mach numbers 4, 7 and 10 and at different angles of attack has led to the following conclusions: An appreciable rise in Mach number and pressure is observable at high speed along the leading edge of a real wing in a region influenced by the interaction of the forebody and the leading edge. At this rise there is a detectable variation in the heat transfer to the surface. In order to predict the heat transfer to the surface it is necessary to account for the influence of pressure gradients in the development of the three dimensional boundary layer. Application of the principle of prevalence permits a method of calculation which for large angles leads to results in agreement with experiment. The experiments made at high Mach number show an influence of entropy gradient due to the curve of the shock wave which causes a variation in the stagnation pressure at the front of the boundary layer.

*Numbers given in the margin indicate the pagination in the original foreign text.

Author

D

1. INTRODUCTION

The study of heat transfer in the stagnation point region of space vehicles can be considered to be well advanced, at least as far as the laminar boundary layer is concerned. A second critical region is less known, however, in the hypersonic glider, namely the wing leading edge, where the prediction concerning the heat transfer to the wall must make use of the analysis of the boundary layer development in the three dimensional flow condition.

The theoretical results presently available concern essentially the case of the slender infinite cylinder. Similarity solutions established by Reshotko and Beckwith (ref. 1) for example, lead to simple formulas for the heat transfer on the stagnation line of the leading edge.

The use however of the formulas for the infinite cylinder, for estimating the heat flux at the leading edge of an actual wing, is questionable for small distances from the nose, because an origin effect can seriously modify the results. These formulas bring no more information on the evolution of the heat transfer in the region where the nose is connected to the leading edge of the wing, and where the pressure and the Mach number can undergo variations which affect in a non negligible way the development of the boundary layer and its essential characteristics.

A study concerning both the theory and the experiment was undertaken in collaboration with the Marseilles Fluid Mechanics Institute and the National Bureau of Aerospace Research and Studies, so that answers to these questions could be found. The present paper extends and terminates the partial analysis published before (ref. 2) and develops theoretical and experimental considerations which were presented in Comptes Rendus of A.S. (refs. 3 and 6).

Experimentally, the program completed was about measurements on the pressure distribution and heat transfer to the wall, along the leading edge of two hypersonic wing models. We recall here the results obtained for different sweep angles at Mach numbers 4, 7 and 10.

Theoretically, two calculation techniques were defined and employed. The first one uses the solution to local equations of the boundary layer and local similarity solutions. The second one uses a solution to the overall energy equation. Both methods utilize the principle of prevalence of the longitudinal flow over the transversal flow in the boundary layer.

2. EXPERIMENTAL

2.1 Test Conditions

2.1.0. The experimental study was made on three wing models of a /2 schematic hypersonic glider, having a spherical sector nose connected to a leading edge of the same radius and two plane faces. The experimental program predicted the pressure readings and the determination of the heat transfer at the wall along the stagnation line (or "stop" line). The models were placed at zero incidence and the leading edge and the skidding varied.

2.1.1. Tests at Mach Nos. 4 and 7. Model A has the following geometrical characteristics: Sweep edge angle: 80°; radius of the nose and the leading edge: 7 mm ($M_\infty = 4$) or 10 mm ($M = 7$). Its overall length is 160 mm ($M_\infty = 4$) or 265 mm ($M_\infty = 7$).

At Mach number 4 the tests were conducted in the supersonic wind tunnel of I.M.F.M. The generator temperature is then close to that of the wall (290° K approximately). The test Mach number is $M_\infty = 3.95$. The generator temperature is adjusted by means of a heater so as to end up having deviations of a few degrees with respect to the temperature of the model (room temperature).

The principle involved in the determination of the transfer of temperautre consists in recording, as a function of time, the rise in temperature of red copper pills of thickness 0.4 mm, inserted inside the brass model and insulated from the latter. The derivative of the temperature with respect to time is read at the initial time of the gust, while the wall temperature is still uniform. Since the model is bulky, its temperature remains practically the same during the gust. After having done these measurements for different values of the ratio T_p/T_i, an essentially linear curve can be drawn, of q/T_i versus T_p/T_i. The slope of this curve $T_i = T_p$ measures the coefficient of flux density of convected heat: $h = \frac{q}{T_p - T_f}$. The ratio T_f/T_i can be determined on this slope for $q = 0$. The sweep edge angles chosen are: 60°, 65°, 70°, 75°, 80°, $85^\circ$and 90°.

At Mach number 7 the tests were made in the hypersonic wind tunnel of I.M.F.M. by Mr. R. Guillaume. The generator temperature was about $600^\circ K$, the wall temperature slightly less than $300^\circ K$. The test Mach number was 7.03.

The principle involved in the determination of the heat transfer is the same as at Mach 4. It is not possible however to change the ratio T_p/T_i sufficiently to obtain a good accuracy in the determination of T_f and h. The thickness of the pills is here 3 mm. The sweep edge angles chosen are 65°, 70°, 75° and 80°.

2.1.2. Tests at Mach Number 10. Model 8 of swept edge angle 75° is made up of a spherical nose and of leading edge of radius 8 mm, and its overall /3 length is 107 mm.

It was tested in the hypersonic wind tunnel R3 of U.N.E.R.A. at Chalais-Meudon, with a test Mach number of $M_\infty = 9.85$. The generator temperature and the wall temperature are on the average $T_i = 1180^\circ K$ and $T_p = 290^\circ K$.

The principle involved in the determination of the heat transferred consists in recording as a function of time the temperature rise of the wall proper, and to deduce from it the heat transferred and the derivative dT/dt. The model made for this has a skin of iron 1 mm thick, whose temperature is measured by means of thermocouples. The derivative of the temperature is taken at the initial time of the gust, a by-pass operation permitting to insure, from this initial time on, the necessary generator temperature. The measured heat fluxes are in this way relative to a uniform wall temperature equal to room temperature.

2.2 Results

2.2.1. Pressure Distribution at the Wall. The experimental study of the pressure was made essentially on the cylindrical part of the leading edge, with the pressures on the spherical part being determined theoretically. A Newtonian law of pressures, extended by a Meyer-Prandth expansion, has been used.

The pressure distributions measured on the stagnation (stop) line of the leading edge are given in figure 1.

At Mach numbers 4 and 7 the lengths of the models are sufficient so that the pressure goes aft to an approximately constant value, close to the pressure that would be obtained for an infinite cylinder in incidence.

The evolution of the pressure at Mach 4, from the distribution observed on the spherical part, occurs in a very regular way, the pressure tends rapidly toward the uniform asymptotic value. The same does not hold at Mach 7; here one can observe near the connection a more irregular evolution, with the pressure going through a minimum which tends to move downstream when the sweep edge angle increases.

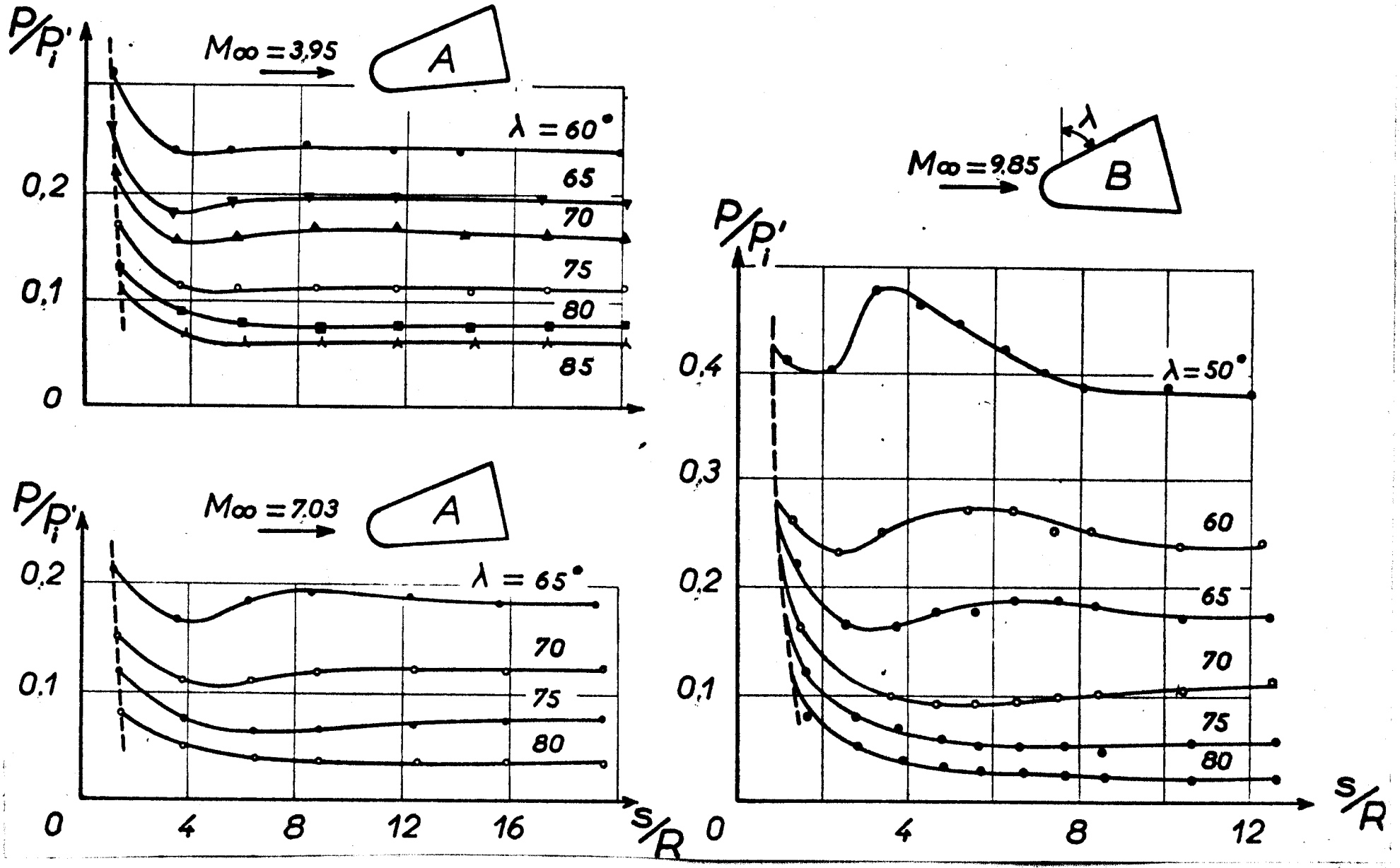

Figure 1. Pressures at the leading edge.

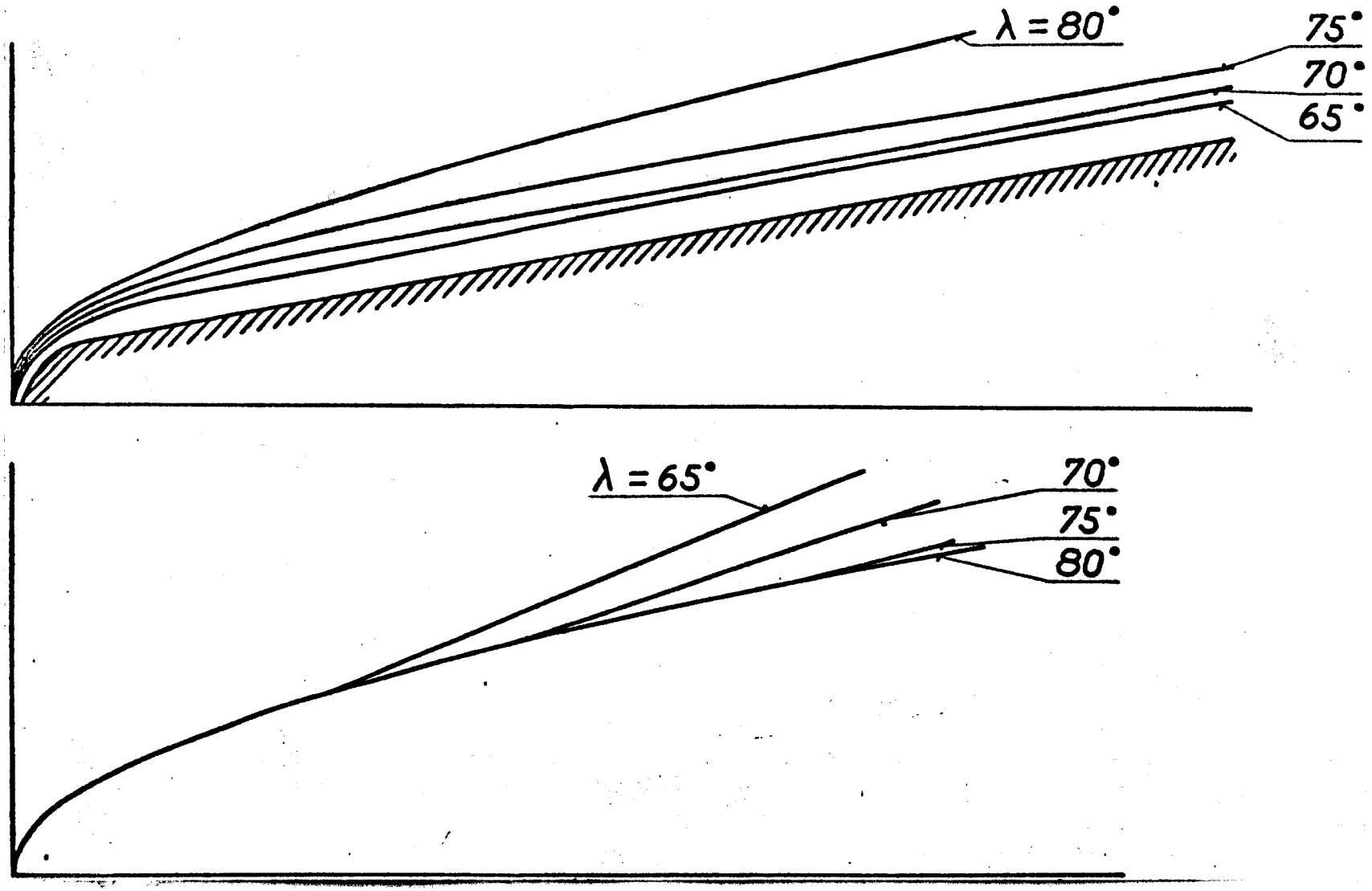

Figure 2. Shock waves at M_∞ = 7.03 [Model A].

This latter phenomenon is still more accentuated at Mach 10. The length of the model employed seems to be insufficient for the asymptotic value of the pressure corresponding to the infinite cylinder to be reached.

2.2.2. Form of the Shock Wave and Entropy Layer. In order to /4 complement the information given by the measurements of pressure, the experimental program has included in all cases an optical study of the shock wave form. A shadowscopic method has been employed to determine with accuracy the trace of the shock wave form. A shadowscopic method has been employed to determine with accuracy the trace of the shock wave on the plane of symmetry. The observation of highly accurate strioscopic lines was made in order to obtain information on the flow mass per unit volume between the leading edge and the shock wave.

Shown, by way of example, is the evolution of the shock wave against the leading edge angle for $M_\infty = 7$. Two types of diagrams were adopted.

In the first type (upper figure) the shock wave form was drawn for a leading edge assumed fixed. One observes quite clearly, for all the sweep edge angles used, that the trace of the shock wave, first superimposed with that of a sphere, comes close to the leading edge, and that this is the more pronounced the smaller the sweep edge angle. The separation distance is observed to be minimum for a sweep edge angle of 65°. This distance seems from then on to go to a constant value at infinity downstream. The fluctuations of the pressure distribution in the neighborhood of the connection are due to the reflection of the expansion waves coming from the wall and originating from the sonic point on the shock wave, on the stream surface (strongly rotational flow), and on the sonic line. In other words these fluctuations are due to the non-viscous effects which are due to the nose bluntness.

In the second type we have shown the different shock waves, with a leading edge no longer fixed but placed at the corresponding sweep edge angles. This configuration permits us to observe the invariance of the sphere's shock wave and also shows the displacement of the beginning of the influence of the cylindrical leading edge.

The strioscopic pictures are shown in figures 3 and 4. They bring additional information by showing that a certain evolution of the mass density takes place between the wall and the shock wave. Two regions are observed between the shock wave and the obstacle. A region of low density shows up in black, is observed near the connection, and expands when the sweep edge angle increases. It seems to identify the high entropy region corresponding to streamlines which have crossed the shock wave near the region's apex. The other region shows up in white and corresponds to streamlines which have crossed the oblique part of the shock wave.

For Mach numbers 7 and 10

In order to better understand the effect, an exploration of pitot pressures was made for Mach number 7 between the wall and the shock wave. Two examples of results obtained at three abscissas are shown in figure 4 on top of the corresponding strioscopic pictures. Since we don't know the static pressures the interpretation of the curves obtained is difficult. Near the coupling with the spherical nose an important evolution of the pitot pressure between the boundary layer edge and the shock wave seems to confirm the crossing of a region whose entropy gradient is very high. Far from the nose, however, a much smaller variation seems to indicate an isentropic flow whose stagnation pressure goes toward the pressure which predominates, downstream of the oblique shock wave from the leading edge.

/5

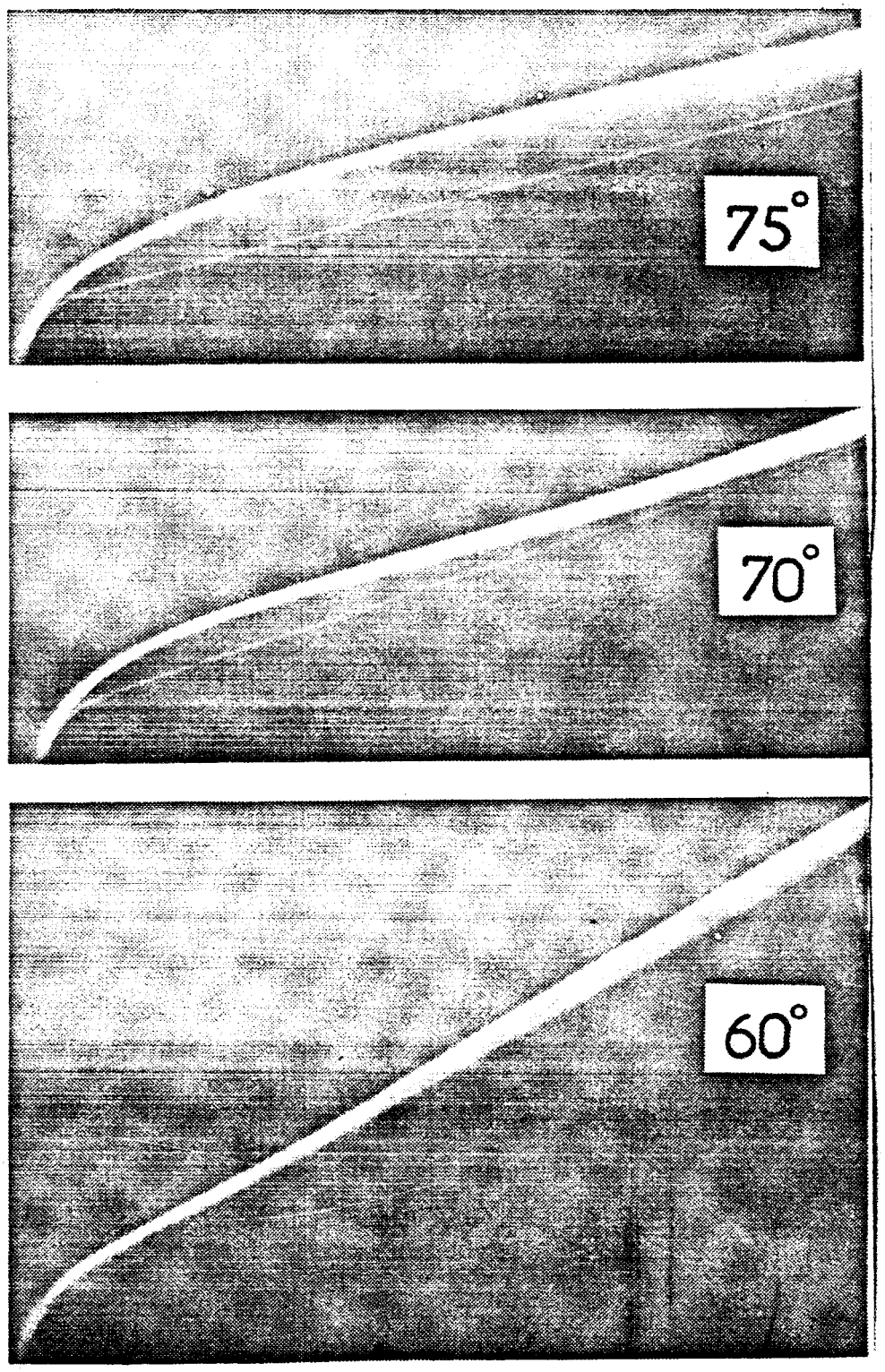

Figure 3. Shock waves at $M_\infty = 9.85$ [Model B].

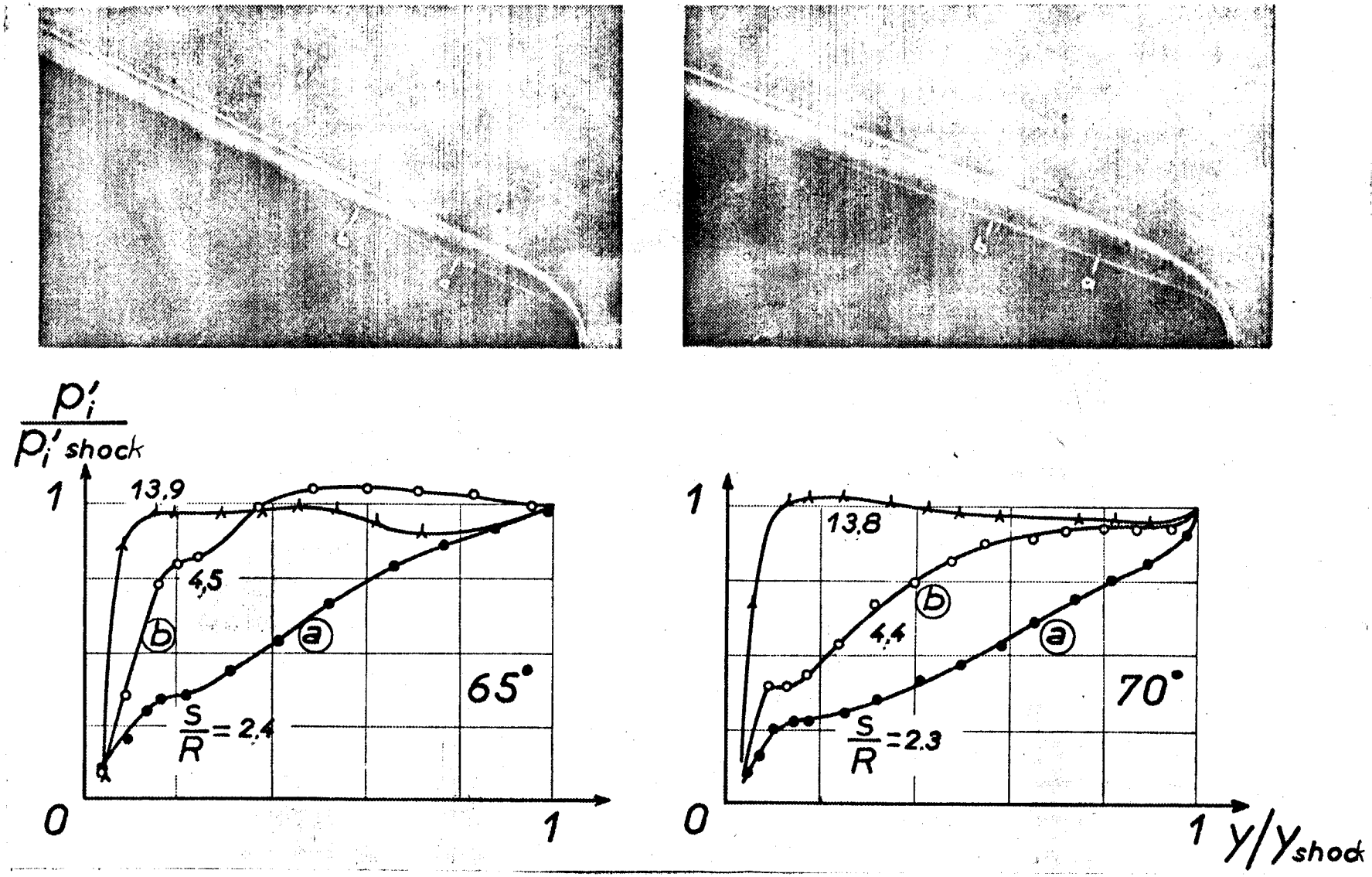

Figure 4. Shock waves and pitot pressures [Model A - M_∞ = 7.03].

It seems therefore that a three-dimensional effect takes place here. The streamlines, which have crossed the shock wave near the apex, go along the leading edge first and then depart from it and go toward the planar faces of the wing. The effect is greater, the higher the sweep edge angle.

2.2.3. Distribution of Heat Flux at the Wall. The results concerning the heat transfers measured along the stagnation line of the leading edge are shown in figures 4, 5 and 6. In all cases the experimental values are referred to the value calculated at the stagnation (stop) point by means of the Fay and Riddell formula.

At Mach number 4 a fairly constant heat transfer is obtained along the cylinder, with its value decreasing when the edge angle increases.

The same does not hold at Mach number 7, as proved in reference 3, nor at Mach 10. The heat flux at the wall undergoes in these cases a more irregular evolution in the sphere-and-cylinder coupling region. This evolution seems directly connected with, as that of the pressure, the above mentioned reflections, with the heat transfer going through a minimum at an abscissa which corresponds approximately to that of the pressure minimum.

3. THEORETICAL STUDY OF THE LAMINAR HEAT TRANSFERS IN THREE-DIMENSIONAL FLOW

3.1. The Prevalence Principle and Form of the General Equations

Various authors, (refs. 4 and 5), have shown that a very important simplification can be made to the three-dimensional boundary layer when the boundary layer velocity component transversal to the external streamline can be assumed small compared to its longitudinal component. This principle of longitudinal flow prevalence, which seems especially applicable to wings of high edge angle, permits to treat the case of the longituidnal flow equations, while it is not

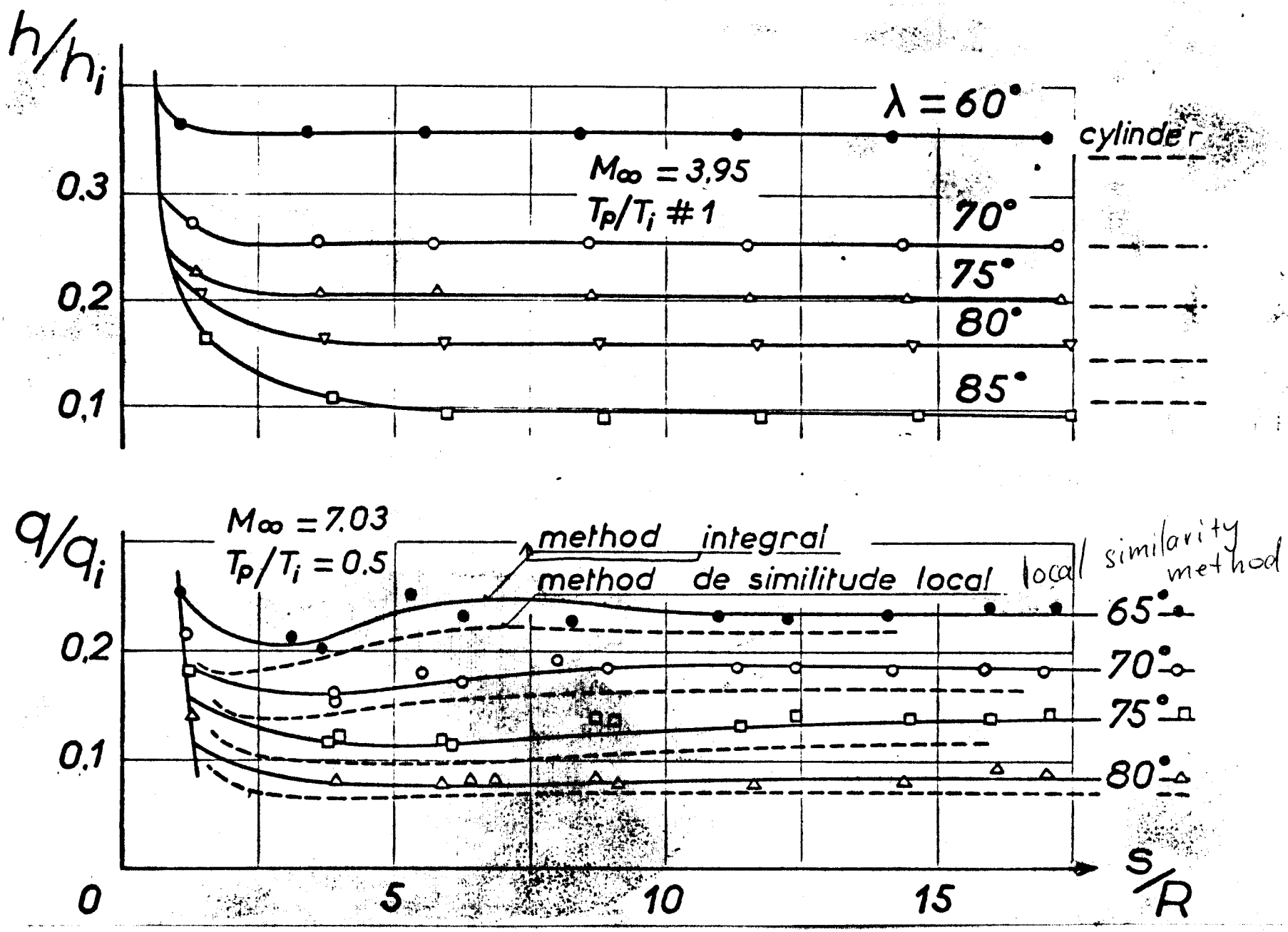

Figure 5. Heat flux at the leading edge of Model A.

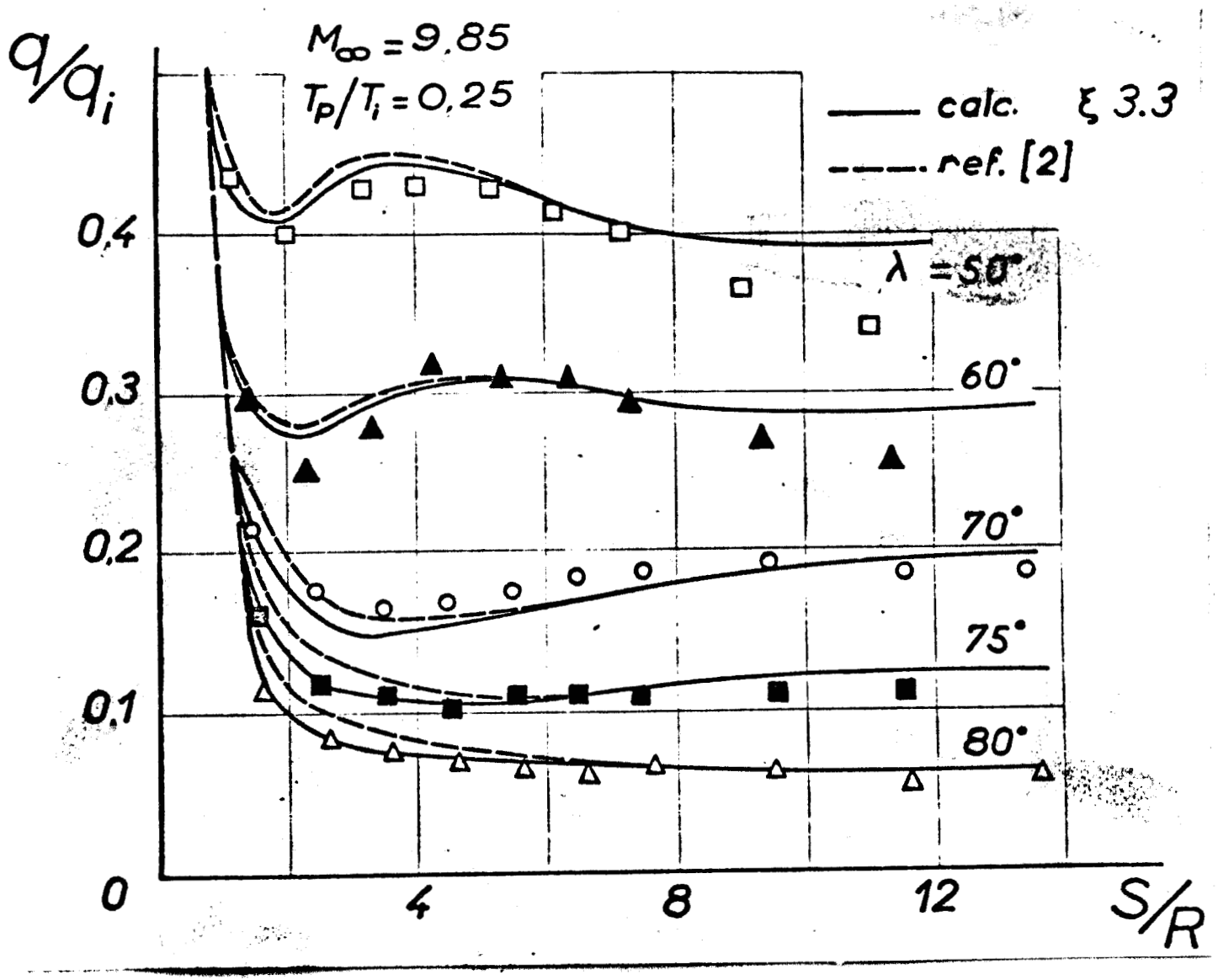

Figure 6. Heat flux at the leading edge of Model B.

necessary to consider the transversal flow equations. Taking for logitudinal axis the projection of the exterior streamline on the surface, the following system of local equations is obtained:

$$\rho u \frac{\partial u}{\partial s} + \rho w \frac{\partial u}{\partial y} = -\frac{\partial p}{\partial s} + \frac{\partial}{\partial y}\left(\mu \frac{\partial u}{\partial y}\right)$$

equation of the log tudinal /6 momentum (1a)

$$\rho u \frac{\partial T_i}{\partial s} + \rho w \frac{\partial T_i}{\partial y} = \frac{\partial}{\partial y}\left[\mu\left(\frac{\partial T_i}{\partial y} + \frac{1 - P_r}{P_r}\frac{\partial T}{\partial y}\right)\right],$$

energy equation (1b)

$$\frac{\partial}{\partial s}(\rho u e) + \frac{\partial}{\partial y}(\rho w e) = 0,$$

continuity equation (1c)

s means the measurements along the streamlines and e, a quantity proportional to the distance between two neighboring streamlines.

The overall equations obtained by integration, along the boundary layer thickness of the momentum and energy local equations, are:

$$\frac{C_f}{2} = \frac{d\delta_2}{ds} + \delta_2\left[\frac{H+2}{u_e}\frac{du_e}{ds} + \frac{1}{\rho_e}\frac{d\rho_e}{ds} + \frac{1}{e}\frac{de}{ds}\right],$$

overall momentum equation (2a)

$$\frac{q}{\rho_e u_e c_p T_{i_e}} = \frac{d\Delta}{ds} + \Delta\left[\frac{1}{u_e}\frac{du_e}{ds} + \frac{1}{\rho_e}\frac{d\rho_e}{ds} + \frac{1}{e}\frac{de}{ds}\right],$$

overall energy equation (2b)

Note immediately that the prevalence principle permits to give the three dimensional boundary layer a form identical to that which would be had by the boundary layer of a body of revolution whose meridian ordinate would be e (s). When the exterior flow of the perfect fluid is known the reduced width e of the streamline pencil is in principle a given quantity of the problem. Any theoretical treatment established for the flow of revolution is then usable in the calculation of the three dimensional boundary layer development.

3.2. Method of Calculating the Heat Transfer to the Wall

3.2.1. Determination of the Streamline Divergence. We propose to establish methods of calculation based on the local equations and on the overall energy equation, using the prevalence principle, with the essential goal being

the prediction of the heat flux at the wall of wings having high edge angles, and especially along their leading edge.

For any method it is necessary to determine the term $1/\varrho \; de/ds$ describing the divergence of streamlines.

For any surface considerations based on differential geometry permit to show that e (s) is a solution of the following differential equation

$$\frac{d^2e}{ds^2} + \left(K + k_2 - \frac{\partial k_2}{\partial n}\right) e = 0 \tag{3}$$

where K is the overall surface curvature and k_2 the geodestic curvature of the streamline at the point under consideration. This latter curvature can be evaluated, provided the distribution of the flow quantities at the edge of the boundary layer is known

(4)

If we take $1/\varrho \; de/ds = \varphi(s)$, we have

$$\frac{d\varphi}{ds} + \varphi^2 = \frac{\partial k_2}{\partial n} - k_2^2 - K \; . \tag{5}$$

Equation (5) is of the first order in φ. The right hand side is generally not known analytically. A step-by-step construction process of streamlines could permit however to make a numerical integration. We have then

$$\left(\exp\left(\int_{s_1}^{s} \varphi(s)\, ds\right)\right) dx = \frac{(s_1)}{(s)}$$

where s_1 is the abscissa of a point where $\varphi(s)$ is arbitrarily chosen. (The function e(s) is found within a multiplicative constant)

In the case of interest to us the overall curvature K is zero on the cylindrical part. The abscissa s_1 will be taken equal to that which corresponds to the connection with the spherical nose. The stagnation (stop) line will be assumed to be a nonsingular streamline ($k_2 = 0$).

Equation (5) becomes

$$\frac{d\varphi}{ds} + \varphi^2 = \frac{\partial k_2}{\partial n} . \tag{6}$$

On the spherical part we can take for e:e = sin s/R.

The initial value of φ at the shoulder is in this way $\varphi(s_1) = \frac{\cot g \Lambda}{R}$.

The derivative $\partial k_2/\partial n$ is generally not known analytically along the separation line. If $\partial k_2/\partial n$ is identically zero, the streamlines near the separation line can be taken as the geodesic lines originating from the stagnation (stop) point. This case can be produced only near $\Lambda = 90^\circ$, and was already studied in reference 6.

For the infinite cylinder we can establish the following relations on the stagnation line

$$\frac{R}{e}\frac{de}{ds} = \frac{R}{u_e}\frac{dv}{dn} \tag{7}$$

$$\frac{\partial k_2}{\partial n} = \left(\frac{R}{u_e}\frac{dv}{dn}\right)^2 \tag{8}$$

These relations are met again at infinity, for the present case of /8 interest. At a finite distance it is necessary however to take into account the origin effect imposed by the connection with the spherical nose, especially in the presence of a pressure evolution. The study proposed in reference 2 uses the relation (7) at a finite distance and is therefore valid only asymptotically.

3.2.2. Method of Local Similarity. As mentioned in the beginning of this chapter, as soon as the prevalence principle is used and the function e (s) known, any theoretical treatment worked out for the flow of revolution can be employed. We have in this way presented in reference 6 the calculation of the transfer for the case where the streamlines merge with the geodesics originating from the point of impact at the edge of the boundary layer, by projection on the surface. The calculation was done by extending the method of Stine and Wanlass (ref. 7), applicable to asymmetrical flows. The method is here extended to the case where e (s) is defined by Equation (6).

The calculation proposed by Stine and Wanlass uses successively the transformations of Mangler and Stewartson and reduces the problem to that of incompressible plane flow. It is then possible to use the similar solutions of the laminar boundary layer of the Falkner-Skan model. The fundamental parameter permitting to establish the local correspondence is $m = s/u_e \; du_e/ds$ which becomes $\bar{m}$ and $\bar{\bar{m}}$ in each of the associated planar flows.

It is then assumed that, to the actual flow at every point, a correspondence can be made with the incompressible planar flow, where the velocity is distributed according to a low of a power of the abscissa, where the exponent is $\bar{\bar{m}}$.

We have in this way, for the local coefficient of heat flux connected to the wall

$$h = k_e \left[\frac{u_e}{\chi_e} \frac{m}{\bar{m}} \frac{\bar{\bar{m}}}{\bar{m}} \left(1 + \frac{\gamma - 1}{2} M_e^2 \right) \left(\frac{\bar{\bar{m}} + 1}{2} \right) \right]^{1/2} \left(\frac{d\theta}{d\eta} \right)_{\substack{\eta = 0 \\ \bar{\bar{m}}}} \qquad (9)$$

where $(d\theta/d\eta)_{\substack{\eta \\ \bar{\bar{m}}}} = 0$ is the temperature gradient at the wall for the corresponding incompressible planar flow.

The parameters $\bar{m}/m$ and $\bar{\bar{m}}/\bar{m}$ are given by $\frac{\bar{\bar{m}}}{\bar{m}} = \frac{\int_0^s e^2 \, ds}{e^2 s}$

$$\frac{\bar{m}}{\bar{m}} = -\left(1 + \frac{\gamma-1}{2} M_e^2\right)^{\frac{5\gamma-3}{2\gamma-1}} \frac{1}{\bar{s}} \int_0^{\bar{s}} \left(1 + \frac{\gamma-1}{2} M_e^2\right)^{-\frac{3\gamma-1}{2(\gamma-1)}} d\bar{s}$$

The reduced temperature gradient $(dB/d\eta)\frac{\eta}{\bar{m}} = 0$ is tabulated for different ratios of T_p/T_i, and for distributions of wall temperatures which can be proportional to a power of $\bar{s}$. /9

The heat transfer q can then be calculated if the recovery factor r is known. The value has been taken equal to $P_r^{1/2}$ for $P_r = 0.7$.

3.2.3. Method Based on the Overall Energy Equation. It was shown (ref 8) that a very flexible method of calculation, based on a solution of the overall momentum equation, permitted to predict with a reasonable degree of approximation the essential dynamic characteristics of a laminar or turbulent boundary layer, for the case of moderate pressure gradients. The approximate method employed here for the heat transfer calculation is the extension of that technique to the overall energy equation.

The fundamental hypothesis employed here in the dynamic problem is to assume that the shape of the velocity and temperature profiles in the boundary layer vary sufficiently little so that the friction coefficient may be expressed by the flat plate relation as a function of the Reynolds number of the momentum thickness. Using the concept of reference temperature, the relation employed for the friction coefficient is

$$\frac{C_f}{2} = \frac{0,2205\, g}{\left(\frac{\rho_e u_e \delta_2}{\mu_e}\right)} \quad \text{with} \quad g = \frac{\rho^* \mu^*}{\rho_e \mu_e} \qquad (10)$$

where g is C_f/C_{f_I} of the laminar flat plate, with R_{δ_2} constant. g is obtained from the mass per unit volume ρ^* and from the viscosity μ^* which corresponds

to the reference temperature T*. It has been proposed to use, for this temperature, the Monaghan relation, as follows

$$T^* - T_e = 0.54\,(T_p - T_e) + 0.16\,(T_f - T_e) \qquad (11)$$

where T_f is the athermal wall temperature having a corresponding recovery factor $r = P_r\ 1/2$.

The same method of treatment is applied now to the overall energy equation, considered as a differential equation of the energy thickness Δ. To integrate the equation, one uses the relation which is an expression of the heat flux at the wall as a function of the Reynolds number of the energy thickness, starting from the properties of the flat plate.

For the laminar flat plate with constant wall temperature there exists a constant ratio between the heat flux coefficient and the fraction coefficient

$$S = Ch \Big/ \frac{C_f}{2} \# P_r^{-2/3}$$

From the relation (10) which is an expression of C_f as a function /10 of $R_{\delta 2}$, one deduces easily, following integration of the overall equations of the flat plate, the relation for the heat flux at the wall as a function of the Reynolds number of the energy thickness.

$$\frac{q}{\rho_e u_e c_p T_{i_e}} = \frac{B}{\left(\frac{\rho_e u_e \Delta}{\mu_e}\right)} \quad \text{with} \quad B = 0.2205\, g\, \left(S \frac{T_p - T_f}{T_{i_e}}\right)^2 \qquad (12)$$

This relation transforms the overall energy equation (2b) into a linear differential equation of order one for Δ^2.

The integration is performed generally from the point s_0 where the energy thickness is known. It yields the following energy thickness

$$(\Delta \rho_e u_e e)^2 = (\Delta \rho_e u_e e)^2_{s_0} + \int_{s_0}^{s} 2 B \rho_e \mu_e u_e e^2 \, ds \, . \qquad (13)$$

The heat flux at the wall is deduced from (13) using (12).

In the problems of interest the starting point of the integration will be the stagnation point of the forebody. The expression for the heat flux ratio at the running point over the stagnation point (stop point) is

$$\frac{q}{q_i} = \frac{\frac{B}{B_i} \frac{\rho_e \mu_e}{\rho_i \mu_i} u_e e}{2 \left[\left(\frac{du_e}{ds} \right)_i \int_0^s \frac{B}{B_i} \frac{\rho_e \mu_e}{\rho_i \mu_i} u_e e^2 \right] ds}^{1/2} \, .$$

3.3. Application to the Leading Edge and Comparison with Experiment

Two regions can be distinguished when applying the calculation to the cases under consideration.

A first region is the spherical sector which makes up the nose whose flow and heat transfer are those of a forebody of revolution. The reduced width of the streamline pencil is here simply proportional to the distance from the wall to the axis which carries the stagnation point and the center of the sphere.

A second region starts from the connection with the cylinder and is the leading edge itself. The problem here is that of a three-dimensional flow having pressure gradients determined by experiment. Taking into account the observations made previously on the origin effect, there is no other /11 possibility available than to take in the calculation for the stagnation

pressure at the edge of the boundary layer, the stagnation pressure p'_i downstream of the right shock detached from the nose. In all cases the experimental curves for the pressure are used in the heat flux calculation.

In reference 2 an approximate relation was used for the divergence of the streamline, as a function of the normal gradient of the velocity and assuming a newtonian transversal pressure distribution

$$\frac{R}{e}\frac{de}{ds} = \frac{R}{u_e}\frac{dv}{dn} = \frac{1}{M_e}\left[\frac{2}{\gamma}\left(1 - \frac{p_\infty}{p_e}\right)\right]^{1/2}.$$

The geometrical study of Section 3.2.1. shows that this relation is in fact rigorous only in the case of a pure cylinder, i.e., at a great distance from the nose.

In the region where the pressure varies, and also close to the connection, the determination of the divergence of streamlines must involve an integration of Equation (6). This integration was made, taking for $\partial k_2/\partial n$, the approximate value

$$\frac{\partial k_2}{\partial n} = \left(\frac{R}{u_e}\frac{dv}{dn}\right)^2$$

which is valid rigorously in the case of a purely cylindrical flow.

On the other hand dv/dn was calculated, under the assumption of a transversal newtonian distribution, from the pressure measured on the stagnation line.

The initial value taken at the shoulder, imposed by the preceding flow of revolution is, as shown in Section 3.2.1.

$$\left[\frac{R}{e}\frac{de}{ds}\right]_{s=s_1} = \operatorname{cotg}\Lambda .$$

At Mach number 4 the fact that the pressure and heat transfer are constant along most of the length of the leading edge has led to using only an asymptotic form of the integral method, namely the form relative to a cylindrical flow at constant pressure and with stagnation pressure p'_i. The corresponding dashed curves drawn on the right of the experimental curves of figure 5 are in fair agreement with the measured values.

At Mach number 7 the calculations have made use of the local and overall methods for the pressure gradient of the leading edge. The corresponding curves, drawn in figure 5 show that each of the two methods shows fairly well the evolution which is experimentally observed, with the flux going through a minimum in the region affected by the connection. It should be noted however that the similarity method involves directly and locally the gradient of the exterior velocity as well as the streamline divergence. The application of this method becomes complicated for wings of average leading edge angle /12 in the region affected by the connection, because of the inaccuracy in the distribution of Mach numbers determined from the pressure at the wall.

Figure 6 shows the results obtained from the application of the integral method to Mach number 10. The method always predicts a minimum of heat flux which approximately corresponds to that of the pressure. A more accurate determination of the streamline pencil width seems in fact to lead to results generally in better agreement with the experiment than those obtained in reference 2.

At high edge angles the experiment and the calculation are in agreement in the whole length of the model. At edge angles of 50° and 60° the experiment is in fairly good agreement with the calculated value but later yields a heat flux which becomes smaller and smaller than the calculated value. The heat flux seems to go toward a new asymptotic value which can be determined by applying the

integral method to a uniform cylindrical flow whose stagnation pressure has the value p_{i_2} of an oblique shock parallel to the leading edge. The results from observations already made on entropy gradient effects due to curvature of the shock wave should be compared.

4. CONCLUSIONS

A theoretical and experimental study of the flow and heat transfer of hypersonic wing leading edges placed under different angles, leads to the following essential conclusions, for Mach numbers 4, 7 and 10:

An appreciable evolution of Mach number and pressure at high velocity is observed along a real wing leading edge, in a region affected by the connection of the forebody with the leading edge proper. Strong variations of heat transfer to the wall are connected with this evolution.

In order to predict the heat transfer at the wall it is necessary to take account of the pressure gradient effects in the development of three-dimensional boundary layer. The application of the principle of prevalence permits to establish methods of calculation which lead at high sweep edge angles to results which are in reasonable accord with experiments.

The experiments performed at high Mach number and at an average sweep edge angle display, however, an influence by the entropy gradients due to the curvature of the shock wave, which in turn leads to a variation of the stagnation pressure at the edge of the boundary layer.

REFERENCES

1. Reshotko, E. and Beckwith, I. E. Compressible Laminar Boundary Layer over a Yawed Infinite Cylinder with Heat Transfer and Arbitrary Prandtl Number. NACA TN 3986, June 1957.

2. Michel, R. and Duong, V. H. Heat Flux at a Highly Swept Wing (Flux de chaleur au bord d'attaque d'une aile en forte flêche). Congrès I.C.A.S. - T.P. O.N.E.R.A. n' 116, 1964.

3. Valensi, J., Guillaume, R., Guffroy, D. and Fraisse, J. P. Influence of the Mach Number and Sweep Angle on the Distribution of Convected Heat Flux Along the Separation Line of the Hemi-cylindrical Leading Edge of a Delta Wing Having a Nose Shaped Like a Spherical Sector, at Zero Incidence (Influence du nombre de mach et de l'angle de flêche sur la distribution du flux de chaleur convectée le long de la ligne de séparation du bord d'attaque hémi-cylindrique d'une aile en delta à pointe en secteur sphérique at sous incidence nulle). C.R.A.S. 259, p. 2174, October 1964.

4. Eichelbrenner, E. A. and Oudart, A. Method of Calculation of the Three-dimensional Boundary Layer (Méthode de calcul de la couche limite tridimensionnelle). Publication O.N.E.R.A. n'76, 1955.

5. Cooke, J. C. and Hall, M. G. Boundary Layers in Three Dimensions (British RAE Rep. Aero 2635).

6. Valensi, J. and Guffroy, D. A Method of Calculating the Local Convection Coefficient (Hypersonic Flows, Three-dimensional Laminar Boundary Layer) (Sur une méthode de calcul du coefficient de convection local (écoulements hypersoniques, couche limite laminaire tridimensionnelle)). C.R.A.S. 259, p. 2344, October 1964.

7. Stine, H. A. and Wanlass, K. Theoretical and Experimental Investigation of Aerodynamic Heating and Isothermal Heat Transfer Parameters on a Hemi-spherical Nose with Laminar Boundary Layer at Supersonic Mach Numbers. NACA TN 3344, December 1954.

8. Michel, B. Turbulent Boundary Layers and Calculation of Boundary Layer of Incompressible Fluids (Couches limites turbulentes et calcul pratique des couches limites en fluide compressible) T.P. O.N.E.R.A. n'25, 1963.